

STPFormer: A State-of-the-Art Pattern-Aware Spatio-Temporal Transformer for Traffic Forecasting

Jiayu Fang, Jessica Shao, Boris Choy and Junbin Gao

University of Somewhere

jiayu.fang@sydney.edu.au

Abstract

Spatio-temporal traffic forecasting is challenging due to complex temporal patterns, dynamic spatial structures, and diverse input formats. Although Transformer-based models offer strong global modeling, they often struggle with rigid temporal encoding and weak space-time fusion. We propose STPFormer, a Spatio-Temporal Pattern-Aware Transformer that achieves state-of-the-art performance via unified and interpretable representation learning. It integrates four modules: Temporal Position Aggregator (TPA) for pattern-aware temporal encoding, Spatial Sequence Aggregator (SSA) for sequential spatial learning, Spatial-Temporal Graph Matching (STGM) for cross-domain alignment, and an Attention Mixer for multi-scale fusion. Experiments on five real-world datasets show that STPFormer consistently sets new SOTA results, with ablation and visualizations confirming its effectiveness and generalizability.

Introduction

With the increasing complexity of transportation systems and diversified road networks, addressing congestion and optimizing routes have become urgent priorities. Although various models have been proposed to tackle these challenges, there is still no unified solution with sufficient generalizability. As a result, prediction errors persist, leading to inefficient fuel consumption, labor misallocation, and sub-optimal infrastructure investment, ultimately causing significant economic losses.

Classical statistical approaches like the Vector AutoRegressive model (Luetkepohl 2005) and Support Vector Regression (Smola and Schölkopf 2004) are interpretable but often rely on restrictive assumptions (e.g., stationarity, node independence) and struggle with nonlinear and spatial dependencies (Zhang and Zhao 1998; Wu, Ho, and Lee 2004). In recent years, Graph Neural Networks (GNNs) have gained attention for modeling spatial relations through message passing (e.g., STGCN, DCRNN, GWN) (Yu, Yin, and Zhu 2018; Li et al. 2018; Wu et al. 2019). Yet, most still depend on fixed adjacency matrices and local aggregation, which can limit their ability to capture long-range or evolving connections.

To overcome these shortcomings, researchers have proposed attention-based architectures. Transformer variants such as STTN (Ma, Zhao, and Hou 2024), GMAN (Zheng et al. 2020a), MTGNN (Wu et al. 2020), and PDFormer (Jiang et al. 2023) use self-attention to learn global dependencies across time and space. However, many still face challenges with rigid time encoding, static spatial assumptions, or weak spatiotemporal integration. Other lines of work, including CNN-based methods (e.g., ST-ResNet) (Zhang, Zheng, and Qi 2016), ODE-inspired designs (e.g., STGODE, STGNCDE) (Fang et al. 2021; Choi and Park 2023), and hybrid models, have made progress but often lack consistency or a unified representation approach.

These models all perform well when carrying out traffic prediction tasks. However, they have a fatal problem, that is, they do not have a strong generalization ability and can quickly adapt to various traffic models in different cities with minimal adjustments. To address these challenges, our team proposed STPFormer, which is a spatio-temporal pattern-aware converter that simulates complex spatio-temporal dependencies through a unified and modular design. This architecture jointly considers temporal evolution, spatial structure and their cross-domain interaction.

To operationalize these patterns, STPFormer integrates four dedicated modules:

- **Temporal Position Aggregator (TPA):** introduces learnable temporal encodings via random-walk embeddings and pattern-key attention, enabling the model to capture diverse and long-range temporal structures.
- **Spatial Sequence Aggregator (SSA):** formulates spatial modeling as a sequential task, using LSTM-augmented attention to learn dynamic, order-aware spatial interactions.
- **Spatial-Temporal Graph Memory (STGM):** facilitates bidirectional alignment between spatial and temporal features, enhancing context propagation and temporal precision.
- **Attention Mixer:** aggregates hierarchical representations from all encoder layers using learnable projection and residual fusion, forming a unified feature space for downstream forecasting.

We validate STPFormer on five benchmark datasets, and the experimental results show that, compared with the com-

peting baselines, STPFormer achieves the most advanced performance and can adapt to various types of data without adjusting parameters. Its accuracy far exceeds that of the existing sota models.

Preliminaries

This section introduces the foundational concepts and mathematical formulations underlying our traffic flow prediction framework.

Problem Formulation

Definition 1 (Road Network as a Graph). A road network is modeled as a directed graph $\mathcal{G} = (\mathcal{V}, \mathcal{E}, \mathbf{A})$, where $\mathcal{V} = \{v_1, \dots, v_N\}$ is the set of N nodes (e.g., sensors or intersections), $\mathcal{E} \subseteq \mathcal{V} \times \mathcal{V}$ is the set of directed edges, and $\mathbf{A} \in \{0, 1\}^{N \times N}$ is the adjacency matrix such that $\mathbf{A}_{ij} = 1$ if there is a directed edge from v_i to v_j .

Definition 2 (Spatio-Temporal Traffic Flow Representation). For a road network \mathcal{G} with N nodes, the traffic flow at time step t is represented as $\mathbf{X}_t \in \mathbb{R}^{N \times d}$, where d denotes the number of traffic features (e.g., speed, volume, occupancy). Over a time horizon T , the complete traffic sequence is encoded as a third-order tensor:

$$\mathcal{X} = \mathbf{X}_{1:T} := [\mathbf{X}_1, \mathbf{X}_2, \dots, \mathbf{X}_T] \in \mathbb{R}^{T \times N \times d}, \quad (1)$$

where the dimensions correspond to time, space, and feature channels, respectively.

Problem Statement Given historical observations $\mathbf{X}_{t-m+1:t} \in \mathbb{R}^{m \times N \times d}$ of m look-back steps at time t over the road network \mathcal{G} , the goal is to predict traffic states for the next h steps, yielding $\hat{\mathbf{X}}_{t+1:t+h} \in \mathbb{R}^{h \times N \times d}$. Formally, the task is to learn a function f that maps historical traffic and topology to future traffic:

$$[\hat{\mathbf{X}}_{t+1}, \dots, \hat{\mathbf{X}}_{t+h}] = f([\mathbf{X}_{t-m+1}, \dots, \mathbf{X}_t], \mathcal{G}), \quad (2)$$

Attention Mechanism

To support our attention-based architecture, we first review the canonical self-attention mechanism, known as scaled dot-product attention. The attention was originally developed for sequence modeling (Vaswani et al. 2017). Given input vectors $\mathbf{X} \in \mathbb{R}^{N \times d}$, queries (\mathbf{Q}), keys (\mathbf{K}), and values (\mathbf{V}) can be formulated as:

$$\mathbf{Q} = \mathbf{XW}_Q, \quad \mathbf{K} = \mathbf{XW}_K, \quad \mathbf{V} = \mathbf{XW}_V, \quad (3)$$

where $\mathbf{W}_{Q,K,V} \in \mathbb{R}^{d \times d_*}$ are learnable parameters for queries, keys, and values. Scaled dot products yield scores and weights:

$$\mathbf{A} = \text{softmax}\left(\frac{\mathbf{Q}\mathbf{K}^\top}{\sqrt{d_k}}\right) \in \mathbb{R}^{N \times N}, \quad (4)$$

and the final output is

$$\mathbf{Y} = \mathbf{AV} \in \mathbb{R}^{N \times d_v}. \quad (5)$$

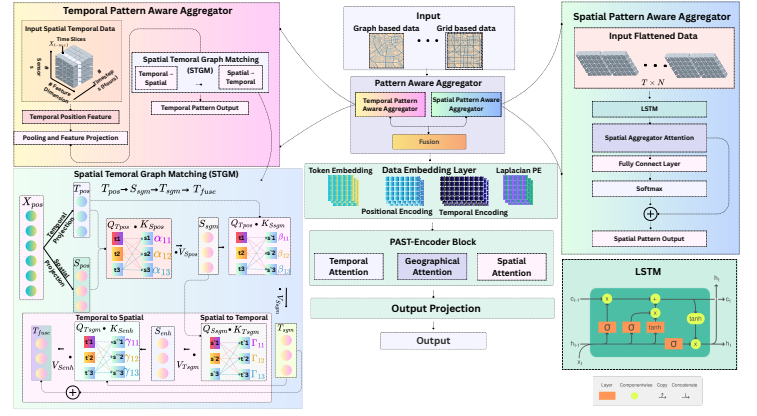


Figure 1: The framework of STPFormer

Methodology

Framework Overview

As shown in Figure 1, STPFormer consists of four key modules that cooperate to model intricate spatiotemporal patterns: (1) a Data Embedding Layer that encodes raw traffic data along with spatial identifiers and temporal indicators; (2) a Pattern-Aware Block, which includes the Temporal Position Aggregator (TPA) and the Spatial Sequence Aggregator (SSA), designed to capture long-range temporal dependencies and dynamic spatial interactions; (3) a Spatial-Temporal Transformer Block, which acts as an Attention Mixer to hierarchically fuse encoder outputs across layers and modalities; (4) an Output Projection Layer that transforms the aggregated features into final traffic predictions.

In the TPA module, we propose a dedicated spatio-temporal Graph Matching (STGM) model to refine temporal representations through bidirectional spatiotemporal alignment. As shown in the bottom-left of Figure 1, each temporal token t and spatial token s is derived via learnable linear projections from the position-enhanced input \mathbf{X}_{pos} . Intermediate representations t' , s' , and s'' correspond to attention-refined features after each stage of message exchange. The four attention maps— α , β , γ , and δ —denote the learned similarity weights for each directional alignment, respectively, and correspond to the formulations in Equations (12)–(15). This design enables STGM to model fine-grained element-wise correlations and effectively capture long-range dependencies across spatial and temporal domains.

Pattern Aware Block

Spatial-Sequence Aggregator (SSA) Traditional graph convolution operations process nodes in a pairwise manner, which often fails to capture broader, corridor-level correlations that span multiple network hops. These long-range spatial dependencies are crucial for understanding traffic flow patterns that extend across entire transportation corridors or ring roads.

To address this limitation, we introduce the Spatial-Sequence Aggregator (SSA), which captures long-range spatial dependencies through a sequential process-

ing approach. Given the spatiotemporal input $\mathbf{X} := \mathbf{X}_{t-m+1:t} \in \mathbb{R}^{m \times N \times d}$ over the past m time steps, the SSA linearizes each $m \times N$ traffic frame into a token sequence:

$$\mathbf{X}_{\text{seq}} = \text{Reshape}_{(mN, d)}(\mathbf{X}), \quad (6)$$

where $\mathbf{X}_{\text{seq}} \in \mathbb{R}^{(m \cdot N) \times d}$ is the flattened spatiotemporal representation treated as a sequence of $m \cdot N$ tokens. The sequential representation is then processed using a combination of LSTM and multi-head attention mechanisms:

$$\mathbf{H}_{\text{SSA}} = \text{LSTM}(\mathbf{X}_{\text{seq}}) + \text{MHAttn}(\mathbf{X}_{\text{seq}}). \quad (7)$$

Here, $\text{LSTM}(\cdot)$ captures sequential dependencies using a standard long short-term memory unit, while $\text{MHAttn}(\cdot)$ applies a multi-head self-attention mechanism to model global interactions across the token sequence. The two outputs are combined via residual addition to obtain the intermediate representation $\mathbf{H}_{\text{SSA}} \in \mathbb{R}^{(m \cdot N) \times d_h}$.

A residual gating mechanism is applied to preserve fine-grained information from the spatiotemporal representation output by the spatial sequence aggregator. Specifically, we define the gated output as:

$$\mathbf{S}_{\text{seq}} = \sigma(\mathbf{W}_g \mathbf{H}_{\text{SSA}}) \odot \mathbf{H}_{\text{SSA}}, \quad (8)$$

where $\mathbf{H}_{\text{SSA}} \in \mathbb{R}^{(m \cdot N) \times d_h}$ is the hidden representation obtained after sequential modeling, $\mathbf{W}_g \in \mathbb{R}^{d_h \times d_h}$ is a shared learnable weight matrix applied to each spatiotemporal token, and $\sigma(\cdot)$ denotes the softmax activation function (as used in our implementation). The gating mechanism $\sigma(\mathbf{W}_g \mathbf{H}_{\text{SSA}})$ controls the flow of information through element-wise multiplication (\odot), enabling the network to selectively retain important features from the original representation \mathbf{H}_{SSA} .

Finally, the processed sequence is reshaped back to the original tensor format: $\mathbf{S} = \text{Reshape}_{(m, N, d_h)}(\mathbf{S}_{\text{seq}})$. The output \mathbf{S} will later be integrated into the Attention Mixer section, where it contributes to the hierarchical aggregation of encoder features, allowing the model to retain and enhance spatial representations across all layers. This design enables the SSA to learn comprehensive spatial patterns such as tidal flows along bus corridors or ring-road traffic dynamics that would be difficult to recover using purely local convolution kernels.

Temporal-Position Aggregator (TPA) Temporal dynamics in traffic systems often exhibit position-sensitive patterns, where certain time steps (e.g., rush hours) carry stronger temporal signals than others. To effectively incorporate such temporal priors, we introduce the Temporal-Position Aggregator (TPA), which enhances temporal representations through positional encoding and structure-aware alignment.

Given the spatiotemporal input $\mathbf{X} \in \mathbb{R}^{m \times N \times d}$ over the past m time steps, we first compress the spatial dimension using average pooling to obtain a temporal sequence. Learnable positional priors are then added:

$$\mathbf{X}_{\text{pos}} = \text{Pool}(\mathbf{X}) + \text{PosEmb}(1 : m). \quad (9)$$

Here, $\text{Pool}(\cdot)$ denotes spatial average pooling across N nodes, and $\text{PosEmb}(1 : m)$ injects learnable random walk-based temporal position embeddings for each time step 1 to m .

The resulting temporal sequence $\mathbf{X}_{\text{pos}} \in \mathbb{R}^{m \times d}$ is then passed through a two-layer feed-forward network (FFN), which maps the input dimension d to a hidden dimension d_h , to transform temporal features. These features are then processed by the Spatial-Temporal Graph Matching module (STGM) for fine-grained alignment:

$$\mathbf{H}_{\text{TPA}} = \text{STGM}(\text{FFN}(\mathbf{X}_{\text{pos}})). \quad (10)$$

The output \mathbf{H}_{TPA} is linearly projected and spatially expanded to form a tensor $\mathbf{T} = \text{Expand}(\mathbf{H}_{\text{TPA}}) \in \mathbb{R}^{h \times N \times d_h}$, restoring the target spatiotemporal shape for prediction. The result \mathbf{T} will later be integrated with result \mathbf{S} of SSA into the Attention Mixer section, where it contributes to attention computation by injecting temporally aligned signals.

This design allows TPA to distinguish position-sensitive time steps and infuse temporal structure into the attention backbone. The core of this temporal alignment is handled by the STGM module, detailed in the following section

Spatial-Temporal Graph Matching Module (STGM) To refine temporal representations with spatial context, we introduce the Spatio-Temporal Graph Matching Module (STGM) as a sub-module within the Temporal Position Aggregator (TPA), which performs bi-directional attention alignment between spatial and temporal projections of the pooled input.

Specifically, the input to STGM is the temporally pooled and position-enhanced sequence $\mathbf{X}_{\text{pos}} \in \mathbb{R}^{m \times d_h}$, produced within the Temporal Position Aggregator (TPA). Two learnable linear projections are applied to \mathbf{X}_{pos} to obtain the temporal and spatial input branches of the module:

$$\mathbf{T}_{\text{pos}} = \mathbf{X}_{\text{pos}} \mathbf{W}_t, \quad \mathbf{S}_{\text{pos}} = \mathbf{X}_{\text{pos}} \mathbf{W}_s, \quad (11)$$

where $\mathbf{W}_t, \mathbf{W}_s \in \mathbb{R}^{d_h \times d_h}$ are learnable projection matrices.

First, we compute attention from \mathbf{T}_{pos} to \mathbf{S}_{pos} to extract temporally guided spatial features. The resulting attention output is concatenated with \mathbf{S}_{pos} and linearly projected to obtain the enhanced spatial representation:

$$\mathbf{S}_{\text{sgm}} = [\mathbf{S}_{\text{pos}}; \text{Attn}_{T \rightarrow S}(\mathbf{T}_{\text{pos}})] \cdot \mathbf{W}_H, \quad (12)$$

where $\mathbf{W}_H \in \mathbb{R}^{2d_h \times d_h}$ is a learnable parameter. The factor 2 arises because the enhanced spatial representation is formed by concatenating the original spatial projection and the temporally guided attention output, effectively doubling the feature dimension before projection back to d_h .

Next, the enhanced spatial features \mathbf{S}_{sgm} are used to guide temporal representation refinement:

$$\mathbf{T}_{\text{sgm}} = \text{Attn}_{S \rightarrow T}(\mathbf{S}_{\text{sgm}}) + \mathbf{T}_{\text{pos}}. \quad (13)$$

Here, $\mathbf{S}_{\text{sgm}}, \mathbf{T}_{\text{sgm}} \in \mathbb{R}^{m \times d_h}$ denote the spatially and temporally enriched representations, respectively.

Temporal-to-Spatial Attention. In the first stage, spatial tokens absorb contextual information from temporal tokens via dot-product attention. Here, \mathbf{S}_{sgm} serves as queries, and \mathbf{T}_{sgm} as keys and values:

$$\mathbf{S}_{\text{enh}} = \text{Softmax}(\mathbf{S}_{\text{sgm}} \mathbf{T}_{\text{sgm}}^\top) \mathbf{T}_{\text{sgm}}. \quad (14)$$

This implements a single-head attention mechanism, where the softmax is applied row-wise across the temporal dimension. The attention map determines how each spatial token attends to temporal cues for context-aware enhancement.

Spatial-to-Temporal Attention. In the second stage, the enhanced spatial features act as a guide to refine temporal representations:

$$\mathbf{T}_{\text{fused}} = \text{Softmax}(\mathbf{T}_{\text{sgm}} \mathbf{S}_{\text{enh}}^\top) \mathbf{S}_{\text{enh}} + \mathbf{T}_{\text{sgm}}. \quad (15)$$

This reversed attention uses \mathbf{T}_{sgm} as queries and \mathbf{S}_{enh} as keys and values, producing a spatially guided temporal output. A residual connection is added to preserve the original temporal signal and improve model stability.

The final output $\mathbf{T}_{\text{fused}} \in \mathbb{R}^{m \times d_h}$ is broadcasted to shape $\mathbb{R}^{m \times N \times d_h}$ and serves as the temporally aligned bias for the Temporal-Position Aggregator (TPA). This dual attention mechanism allows spatial context to guide the refinement of temporal structures, enhancing the modeling of fine-grained traffic dynamics. The final output $\mathbf{T}_{\text{fused}}$ is part of TPA and will be returned according to Equation (10). To be consistent, we write the output $\mathbf{T}_{\text{fused}}$ as \mathbf{H}_{TPA} .

Data Embedding Layer

In the Spatial Graph Embedding (Jiang et al. 2023), spectral graph theory is used to generate a global structure-aware embedding for each time step t , formulated as $\mathbf{X}_{t,\text{spe}} = \mathbf{U}_{\text{spe}} \mathbf{W}_{\text{spe}} + \mathbf{b}_{\text{spe}}$, where \mathbf{U}_{spe} consists of the top- k eigenvectors of the Laplacian matrix, capturing the road network topology. For the Temporal Periodic Embedding, periodic traffic cycles are encoded by decomposing each timestamp t into a weekly index $w(t)$ and a daily index $d(t)$, which are embedded as $\mathbf{X}_w, \mathbf{X}_d \in \mathbb{R}^{m \times d}$ to capture multi-scale temporal patterns consistent with the spatial features (Jiang et al. 2023). For the Temporal Positional Encoding, the absolute position of each timestamp is represented using a sinusoidal encoding (Vaswani et al. 2017): $\mathbf{X}_{t,\text{tpe}}(i) = \sin(\frac{t}{10000^{2i/d}})$ for even i and $\cos(\frac{t}{10000^{2(i-1)/d}})$ for odd i , forming the matrix $\mathbf{X}_{\text{tpe}} \in \mathbb{R}^{m \times d}$, which provides continuous position-aware information. Finally, the Embedding Integration step combines all components through element-wise summation with appropriate broadcasting. The unified embedding $\mathbf{X}_{\text{emb}} \in \mathbb{R}^{m \times N \times d}$ is computed as:

$$\mathbf{X}_{\text{emb}} = \mathbf{X}_{\text{data}} + \mathbf{X}_{\text{spe},t} + \mathbf{X}_{w,n} + \mathbf{X}_{d,n} + \mathbf{X}_{\text{tpe},n}, \quad (16)$$

where $\mathbf{X}_{\text{spe},t} \in \mathbb{R}^{N \times d}$ is broadcast along the temporal axis, while $\mathbf{X}_{w,n}, \mathbf{X}_{d,n}, \mathbf{X}_{\text{tpe},n} \in \mathbb{R}^{m \times d}$ are broadcast across spatial nodes. For clarity, we denote $\mathbf{X} \equiv \mathbf{X}_{\text{emb}}$ hereafter.

Pattern Aware Spatial Temporal Encoder Block (PAST-Encoder Block)

The Pattern-Aware Spatio-Temporal Encoder comprises three attention blocks: temporal attention, geographical attention, and spatial attention, which process the inputs \mathbf{X}_t and \mathbf{X}_n , respectively. This design follows the approach proposed in (Jiang et al. 2023). An example of the spatial attention mechanism at each time step t is illustrated as follows: $\mathbf{Q}_t = \mathbf{X}_t \mathbf{W}_Q$, $\mathbf{K}_t = \mathbf{X}_t \mathbf{W}_K$, and $\mathbf{V}_t = \mathbf{X}_t \mathbf{W}_V$,

where $\mathbf{W}_Q, \mathbf{W}_K, \mathbf{W}_V \in \mathbb{R}^{d \times d_0}$ are learnable matrices and d_0 is the hidden dimension. Spatial, geometrical and temporal self-attention are then computed as the following respectively:

$$\mathbf{X}_t^{\text{spat}} = \text{Softmax}\left(\frac{\mathbf{Q}_t \mathbf{K}_t^\top}{\sqrt{d_0}}\right) \mathbf{M}_{\text{spat}}, \quad (17)$$

$$\mathbf{X}_t^{\text{geo}} = \text{Softmax}\left(\frac{\mathbf{Q}_t \mathbf{K}_t^\top}{\sqrt{d_0}}\right) \mathbf{M}_{\text{geo}}, \quad (18)$$

$$\mathbf{X}_n^{\text{temp}} = \text{Softmax}\left(\frac{\mathbf{Q}_n \mathbf{K}_n^\top}{\sqrt{d_0}}\right). \quad (19)$$

Here, \mathbf{M}_{spat} and \mathbf{M}_{geo} are binary spatial and geographical masking matrices, respectively, which assign a weight of 1 to the connections between a node and its spatial or geographical neighbors, and 0 otherwise. The outputs from the geo-heads, spatial-heads, and temporal-heads of the multi-head attention are concatenated and then projected through a shared linear transformation:

$$\text{PAST-Encoder} = \bigoplus \left(\mathbf{X}_{1,\dots,h_{\text{geo}}}^{\text{geo}}, \mathbf{X}_{1,\dots,h_{\text{spat}}}^{\text{spat}}, \mathbf{X}_{1,\dots,h_{\text{temp}}}^{\text{temp}} \right) \mathbf{W}^O, \quad (20)$$

where \bigoplus denotes the concatenation along the head dimension, $h_{\text{geo}}, h_{\text{spat}}, h_{\text{temp}}$ are the number of heads for geographical, spatial, and temporal attention respectively, and $\mathbf{W}^O \in \mathbb{R}^{d \times d}$ is a learnable output projection matrix. Finally, the output of this multi-head self-attention is fed into a position-wise feed-forward network to obtain the updated representation $\mathbf{H}^{(l)} \in \mathbb{R}^{m \times N \times d}$.

Attention Mixer and Output Layer

Attention Mixer The Attention Mixer integrates multi-perspective spatio-temporal features and performs hierarchical attention-based refinement. It begins by constructing an enhanced embedding \mathbf{X}_{mix} through the element-wise addition of the raw input \mathbf{X} embedding, the temporal-aware bias \mathbf{T} from the Temporal Position Aggregator (TPA), and the spatial-aware representation \mathbf{S} from the Spatial Sequence Aggregator (SSA):

$$\mathbf{X}^{\text{mix}} = \text{Embed}(\mathbf{X}) + \mathbf{T} + \mathbf{S}. \quad (21)$$

This fused representation $\mathbf{X}_{\text{mix}} \in \mathbb{R}^{m \times N \times d_h}$ is then processed by a stack of L encoder blocks, each designed to capture complex temporal and spatial patterns. Specifically, \mathbf{X}^{mix} is split into temporal $\mathbf{X}_n^{\text{mix}}$ and spatial $\mathbf{X}_t^{\text{mix}}$ and then feed into the PAST-EncoderBlock, and correspond to the formulations in Equations (18)–(20). In here, each encoder block incorporates attention-based modules—including multi-head self-attention and pattern-aware matching—to refine spatio-temporal representations:

$$\mathbf{H}^{(l)} = \text{PAST-EncoderBlock}^{(l)}(\mathbf{X}_{\text{mix}}), \quad l = 1, \dots, L. \quad (22)$$

To align feature formats across all encoder layers, the outputs $\mathbf{H}^{(l)} \in \mathbb{R}^{m \times N \times d_h}$ are permuted and projected via learnable 1×1 convolutions:

$$\mathbf{M}^{(l)} = \text{Conv}_{1 \times 1}^{(l)}(\text{Permute}(\mathbf{H}^{(l)})). \quad (23)$$

Here, $\mathbf{M}^{(l)} \in \mathbb{R}^{d_h \times N \times m}$. The projected multi-level outputs are then aggregated by residual summation to obtain the final

mixed spatio-temporal feature representation:

$$\mathbf{S}_{\text{mix}} = \sum_{l=1}^L \mathbf{M}^{(l)}. \quad (24)$$

By combining fused embeddings with multiple attention-enhanced encoder layers, the Attention Mixer facilitates deep integration of spatial and temporal patterns across multiple levels. The resulting tensor \mathbf{S}_{mix} is passed into the output module for traffic forecasting.

Output Layer The output layer transforms the aggregated spatio-temporal feature tensor $\mathbf{S}_{\text{mix}} \in \mathbb{R}^{d_h \times N \times m}$ into the final prediction. It first applies a point-wise 1×1 convolution to project the channel dimension to the output feature size d_{out} , followed by a second convolution to reshape the temporal axis into the forecasting horizon h :

$$\hat{\mathbf{Y}} = \text{Conv}_{\text{out}}(\text{ReLU}(\text{Conv}_{1 \times 1}(\mathbf{S}_{\text{mix}}))). \quad (25)$$

Here, $\hat{\mathbf{Y}} \in \mathbb{R}^{d_{\text{out}} \times N \times h}$ is the predicted traffic state over the forecast horizon. This design preserves spatial structure while enabling flexible output generation across various prediction tasks.

Experiment

We evaluate our model on five benchmark traffic datasets, PeMS04, PeMS07, PeMS08, NYCTaxi, and CHIBike, spanning diverse spatio-temporal patterns and accessible via the LibCity repository (Wang, Jiang, and Jiang 2023).

Datasets and Experiment Setup

Table 1: Dataset Information

Dataset	Nodes	Edges	Seps	Interval	Time Range
PeMS04	307	340	16992	5 min	01/01/2018 – 02/28/2018
PeMS07	883	866	28224	5 min	05/01/2017 – 08/31/2017
PeMS08	170	295	17856	5 min	07/01/2016 – 08/31/2016
NYCTaxi	75 (15×5)	484	17520	30 min	01/01/2014 – 12/31/2014
CHIBike	270 (15×18)	1966	4416	30 min	07/01/2020 – 09/30/2020

Datasets The freeway datasets PeMS04, PeMS07, and PeMS08 capture 5-minute traffic volumes collected by Caltrans loop detectors; each sensor is represented as a graph node and edges follow physical road connectivity, with PeMS07 being the most extensive (883 nodes, 866 edges) (Song et al. 2020). NYCTaxi provides 30-minute taxi demand on a 15×5 Manhattan grid but lacks an explicit spatial graph, requiring models to infer latent spatial dependencies (Liu et al. 2020). CHIBike contains 30-minute rental counts from 270 bike stations projected onto a 15×18 grid and features sparse, irregular, and spatially imbalanced demand (Vaswani et al. 2017).

Experiment Setup Training is performed on a virtualized GPU (vGPU 48GB). We set the batch size to 16 across all experiments. The model is trained using the AdamW optimizer with an initial learning rate of 0.001, a cosine learning rate scheduler, and a 5-epoch warm-up phase. Early stopping is applied based on validation loss with a patience of

50 epochs. A fixed random seed (seed=1) is set for Python, NumPy, and PyTorch to ensure the reproducibility of results. All results are reported based on a single run unless otherwise stated.

Experimental Results and Analysis

Table 2: Performance on state-based Datasets.

Model	PeMS04			PeMS07			PeMS08		
	MAE	MAPE(%)	RMSE	MAE	MAPE(%)	RMSE	MAE	MAPE(%)	RMSE
VAR	23.750	18.090	36.660	101.200	39.690	155.140	22.320	14.470	33.830
SVR	28.660	19.150	44.590	32.970	15.430	50.150	23.250	14.710	36.150
DCRNN	22.737	14.751	36.575	21.132	11.282	36.513	18.185	11.215	27.122
STGCN	21.758	13.874	34.769	22.898	11.983	35.440	17.134	11.211	27.125
GWNET	19.358	13.001	31.646	21.121	10.991	34.328	15.377	9.584	24.122
MTGNN	19.076	12.961	31.564	20.284	9.032	34.987	12.396	10.170	23.713
STSGCN	21.185	13.882	34.678	21.064	10.847	34.376	14.671	10.117	23.861
STFGRNN	19.830	13.021	31.870	21.022	9.212	33.805	14.063	10.547	24.531
STGODE	20.849	13.781	33.151	22.976	10.274	37.043	16.819	10.157	25.446
STGN-CDE	21.019	12.772	31.581	22.060	8.864	34.276	14.559	9.241	23.711
STTN	19.478	13.631	31.910	21.344	9.674	34.487	13.534	10.118	23.491
GMAN	19.139	13.193	31.490	21.066	9.271	34.124	13.561	9.654	23.715
TFormer	18.916	12.711	31.349	20.754	9.627	34.062	12.991	9.144	24.851
ASTGNN	18.601	12.630	31.074	21.070	9.134	34.615	13.119	9.144	24.710
PDFormer	18.321	12.103	29.965	19.832	8.529	32.870	13.583	9.046	23.505
DTRformer	18.005	11.886	29.657	20.202	8.673	33.211	13.181	8.860	22.874
Ours	17.525	11.580	28.941	18.727	8.054	30.919	12.796	8.530	22.006

We compare STPFormer (ours) against diverse baselines on both sensor-based (PeMS04/07/08) and grid-based (NYCTaxi, CHIBike) datasets, using MAE, MAPE, and RMSE as metrics (Table 2, Table 3). Key observations are as follows:

(1) The statistical models (VAR, SVR) lack clear spatial structure modeling, so their performance is relatively poor, especially on PeMS08. However, the data of STPFormer(our) is excellent, being 12.796.

(2) The classic GNN-based methods (GWNET, STGCN, STSGCN) assume static topological structures. While STPFormer (our) dynamically models spatial dependence, compared with STGCN, the MAE of NYCTaxi inflow is reduced by 33.7%, and it achieves lower errors than the recent sota model DTRFormer.

(3) Advanced GNNS (MTGNN, STGN-CDE) perform poorly in irregular grids. STPFormer (ours) has achieved stronger generalization than traditional gnn and DTRFormer.

(4) Attention-based models (ASTGNN, STTN) may overfit sparse regions. STPFormer (our) enhances long-term dependency capture and achieves the best MAE and RMSE on CHIBike inflows, which are 0.365 and 1.381 respectively.

(5) Models based on cnn (STResNet, DSAN, DMSST-Net) usually do not have time alignment and remote memory designed. STPFormer (our) demonstrates the ability of sota in both dense grids and sparse sensor networks.

Ablation Study

We conduct ablation studies on PeMS08 and NYCTaxi to evaluate three forms: (i) w/o TPA & STGM, (ii) w/o STGM, and (iii) the full STPFormer (ours). Figure 2 shows that removing TPA and STGM will lead to very high errors. Adding TPA will improve this result, and the complete STPFormer (our) shows the performance of sota on both datasets.

Table 3: Performance on state-based Datasets..

Models	NYCTaxi						CHBike					
	MAE	inflow MAPE(%)	RMSE	MAE	outflow MAPE(%)	RMSE	MAE	inflow MAPE(%)	RMSE	MAE	outflow MAPE(%)	RMSE
STResNet	14.492	14.543	24.050	12.798	14.368	20.633	4.767	31.382	6.703	4.627	30.571	6.559
DMSTNet	14.377	14.214	23.734	12.566	14.218	20.409	4.687	32.113	6.635	4.594	31.213	6.455
DSAN	14.287	14.208	23.585	12.462	14.272	20.499	4.612	31.621	6.695	4.495	31.256	6.367
DCRNN	14.421	14.353	23.876	12.828	14.344	20.067	4.236	31.264	5.992	4.211	30.822	5.824
STGCN	14.377	14.217	23.860	12.547	14.095	19.962	4.212	31.224	5.954	4.184	30.782	5.779
GWNET	14.310	14.198	23.799	12.282	13.685	19.616	4.159	31.193	5.947	4.101	30.690	5.693
MTGNN	14.194	13.984	23.696	12.272	13.682	19.563	4.112	31.148	5.987	4.086	30.561	5.669
STGCN	15.004	15.203	26.191	13.233	14.698	21.651	2.526	32.993	5.941	4.265	32.612	5.879
STFGNN	15.336	14.869	26.112	13.178	14.584	21.627	4.143	32.222	5.933	4.264	32.321	5.698
STGODE	14.621	14.793	25.444	12.834	14.398	20.205	4.169	31.165	5.921	4.125	30.726	5.698
STGCNDE	14.281	14.171	23.742	12.762	13.681	19.608	4.033	31.195	5.913	4.094	30.595	5.678
STTN	14.359	14.206	23.841	12.373	13.762	19.827	4.160	31.208	5.932	4.118	30.704	5.723
GMAN	14.267	14.114	23.728	12.273	13.672	19.594	4.171	31.155	5.910	4.090	30.662	5.675
TFormer	13.995	13.912	23.487	12.211	13.611	19.522	4.071	31.144	5.878	4.037	30.647	5.638
ASTGNN	13.844	13.692	23.177	12.112	13.602	19.402	3.998	31.181	5.818	3.981	30.617	5.609
PDFormer	13.152	12.743	21.957	11.575	12.820	18.394	3.950	30.214	5.559	3.837	29.914	5.402
DTRFormer	11.343	10.886	20.124	10.201	11.221	17.675	2.975	30.004	5.332	2.765	30.297	5.453
Ours	9.539	9.000	18.417	9.064	10.002	16.125	0.365	29.982	1.381	0.350	29.662	1.337



Figure 2: Ablation study on PeMS08 and NYCTaxi.

PeMS08 (State-based). This dataset has strong periodicity and spatial heterogeneity. As shown in Figure 3(a), (w/o TPA & STGM) can lead to relatively high spatiotemporal errors, especially during peak periods, such as the error between 60 and 100 nodes. Its output (c) differs significantly from the daily cycle, indicating that modeling time dependence using only the Spatial Sequence Aggregator (SSA) is not ideal. Using the time-location aggregator (w/o STGM), the error decreased significantly in the high-variance region (g), and time alignment improved the predictions with time steps ranging from 4 to 10 and nodes ranging from 60 to 100 (h). The output (i) of (w/o STGM) is more stable than that of (w/o TPA & STGM). Adding the Spatial Temporal Graph Matching module (STGM) further enhances the performance of the model: the errors of edge nodes are significantly reduced, such as nodes 12 and 288, graph (m). The final output (o) of STPFormer (ours) shows superior spatiotemporal consistency, verifying the complementary role of all integrated modules.

NYCTaxi (Grid-based). Unlike PeMS08, the characteristics of NYCTaxi are high spatial variability and weak temporal periodicity. As shown in Figure 3 (d), the form of (w/o TPA & STGM) presents dispersed high-error regions, especially in the central and lower grid positions, such as 30 to 50 and 60 to 75. The output (f) is unstable in time and inconsistent in space, which indicates that it is not ideal to use the Spatial Sequence Aggregator (SSA) alone to process grid structures and irregular data. After adding the Temporal Position Aggregator (TPA) (j), there is a significant improvement in the middle grid area. The improved heatmap (k) shows that the improvement is local and sparse, indicating that the temporal consistency remains unsatisfactory. In contrast, the form (l) without the spatio-temporal graph matching module shows a more organized structure, but there are still some deficiencies. After merging the spatio-temporal graph matching module, STPFormer achieved greater improvement: The error graph (p) became smoother, and the errors in areas 25 to 45 and 66 to 78 were significantly reduced. Furthermore, the improved graph (q) demonstrates that integrating spatial memory can significantly enhance the model. The final prediction output (r) of STPFormer (ours) maintains a high degree of spatiotemporal consistency and captures the urban taxi traffic patterns more accurately.

Visual of Data Transformations Across Modules

To analyze the contributions of each module, we visualize the intermediate output of PeMS08 and NYCTaxi. These two datasets are different in spatial structure. STPFormer (ours) is always learning meaningful spatiotemporal patterns between the two.

PeMS08 (State-based). As shown in Figure 4, the original input (a) is sparse and fragmented. After using the Pattern module (b), the vertical time pattern becomes clearer and the signal distribution is more uniform, which means that the Pattern module can better capture repetitive trends. Temporal Position (TPA) (c) helps keep the time series more consistent by connecting points over a longer period of time. For the Spatial Sequence Aggregator (SSA) input (g), we

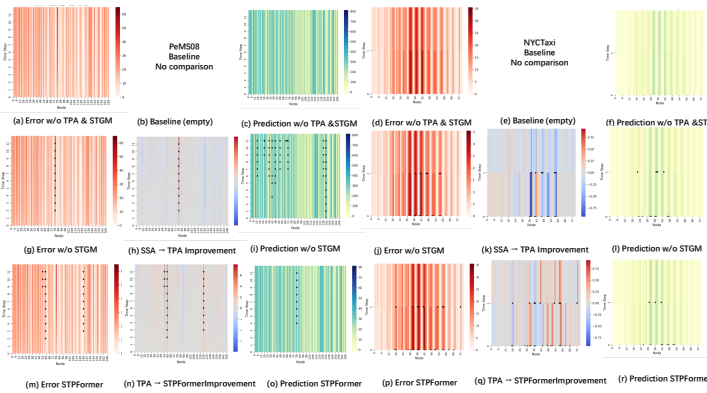


Figure 3: Ablation of model on PeMS08 and NYCTaxi.

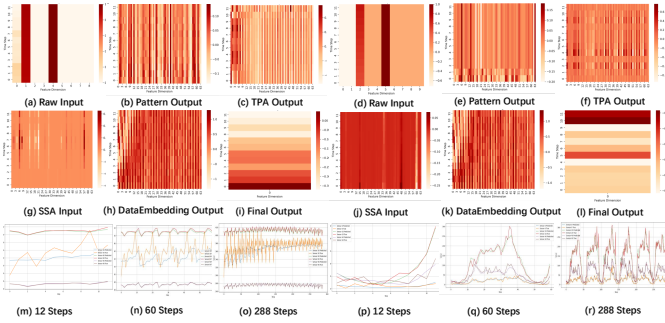


Figure 4: Visualization of module output and time steps.

can observe the process of adding local spatial information. Although the data layout is sparse, the important links between the data are retained. Data Embedding output (h) adds additional information, such as the time of day, making the signal denser and smoother over time. Finally, the results of STPFormer (our) (i) show clear and well-organized patterns, and become smoother over time. The prediction results (m-o) verify the robustness of STPFormer (our) at all levels. The predictions for the short term (12 hours and 60 steps) and the long term (288 steps) are both very close to the real data, proving that the model has a very strong generalization ability in the daily traffic.

NYCTaxi (Grid-based). As shown in Figure 4, the original input (d) indicates that most of the features are sparse and of low variation, which means that the appearance of taxis is very uneven and concentrated in certain areas. Unlike the PeMS08 data, NYCTaxi does not have a clear road network structure, but there are strong regional differences. For instance, the downtown area is very active, while many other places have almost no demand. The Spatial Sequence Aggregator (SSA) (j) learns spatial dependencies without an explicit adjacency graph, identifying correlated grids and filtering noise in inactive areas. The Data Embedding (k) injects position-aware features, helping distinguish spatially similar but functionally distinct grids, like similar volume but different peak hours. The final output (l) shows the predicted taxi demand for each future time step. This illustrates how STPFormer (ours) turns the complex spatio-temporal features it learns into clear and understandable demand. The Prediction Curve (p-r) clearly indicates that for short-term predictions, the model closely follows the actual trend, while for longer-term predictions, the model still maintains a smooth transition under sudden changes. This proves that even when the requirements change greatly and there is no clear spatial structure, this model can still work well.

Combined with the results of PeMS08, STPFormer (ours) can transform the original data into clear and consistent spatiotemporal patterns. For PeMS08, TPA helps to better align the time series, and SSA makes the structure smoother. Take NYCTaxi as an example. The results show that STPFormer (ours) can effectively handle different types of traffic data and has a strong generalization ability.

Related Work

Traffic forecasting is challenging because it must capture complex patterns in both space and time, often under irregular and dynamic conditions. Traditional statistical methods, such as ARIMA (Zhou, He, and Sun 2006) and the Vector AutoRegressive model (Luetkepohl 2005), rely on assumptions of linearity and stationarity, which limit their flexibility in practice. Deep learning models, including CNNs (Krizhevsky, Sutskever, and Hinton 2012) and RNNs (Lv et al. 2015), can learn nonlinear relationships but often treat spatial and temporal features separately, but they dealt with it independently.

Graph Neural Networks (GNNs) improve spatial modeling by leveraging topological information. Models like DCRNN (Li et al. 2018) and STGCN (Zhang, Zheng, and Qi 2016) have shown promising results but depend on static graphs and fixed temporal windows, which can restrict adaptability. Later models, such as MTGNN (Wu et al. 2020) and DGCRN (Li et al. 2023), use adaptive graphs and dynamic connections, yet they often still face challenges in fully modeling temporal patterns and smoothly integrating spatial and temporal contexts. Attempts like DFormer (Zhao et al. 2024) aim to couple spatial and temporal components more tightly.

The transformer structure has indeed performed outstandingly in practice due to its own excellent characteristics, such as the global acceptance domain and modeling flexibility, such as GMAN (Zheng et al. 2020b), STTN (Ma, Zhao, and Hou 2024), and AutoST (Pan et al. 2021) adapt vanilla Transformers to spatiotemporal data but it has also been criticized by researchers for using static spatial graphs or fixed-position encoding. Recent methods like STFormer (Qin et al. 2021) and DGFormer (Xu et al. 2024) introduce adaptive attention on learned graph structures but remain tailored to either state-based or grid-based data. Hybrid approaches, including PDFFormer (Jiang et al. 2023), CCDSReFormer (Shao et al. 2024b) and ST-LLMDF (Shao et al. 2024c) improve flexibility but can struggle with interpretability or input heterogeneity.

Recently, selective state space models have emerged as a powerful alternative for spatiotemporal forecasting due to their linear complexity and ability to handle long-range dependencies. Models such as ST-Mamba (Shao et al. 2024a), STDAAtt-Mamba (Shao et al. 2025b), and ST-MambaSync (Shao et al. 2025a) integrate selective state space dynamics with spatial attention mechanisms to capture both local and global structures. These architectures enhance interpretability while maintaining competitive accuracy but lacks an inherent mechanism to model spatial dependencies, which are essential for accurately capturing the localized interactions between nodes.

To address these gaps, we propose a unified architecture that integrates multi-scale spatiotemporal learning through the Temporal Position Aggregator (TPA) and Spatial Sequence Aggregator (SSA). Together, these modules jointly capture latent dynamics and cross-domain dependencies in both sensor- and grid-based traffic scenarios.

Conclusion

We present STPFormer, a unified spatiotemporal forecasting framework that models complex dependencies across space and time. It combines a Temporal Position Aggregator (TPA), Spatial Sequence Aggregator (SSA), and Spatial-Temporal Graph Memory (STGM) to align temporal and spatial features more effectively, while an Attention Mixer fuses multi-scale information within the encoder. Unlike existing models with static encodings or separate blocks, STPFormer adapts dynamically to diverse traffic conditions. Experiments on five real-world datasets with varying traffic modes show that STPFormer consistently outperforms strong baselines for both sensor-based and grid-based forecasting, demonstrating its robustness and generalization.

References

Choi, J.; and Park, N. 2023. Graph Neural Rough Differential Equations for Traffic Forecasting. *ACM Trans. Intell. Syst. Technol.*, 14(4).

Fang, Z.; Long, Q.; Song, G.; and Xie, K. 2021. Spatial-Temporal Graph ODE Networks for Traffic Flow Forecasting. In *Proceedings of the 27th ACM SIGKDD Conference on Knowledge Discovery & Data Mining*, KDD '21, 364–373. New York, NY, USA: Association for Computing Machinery. ISBN 9781450383325.

Jiang, J.; Han, C.; Zhao, W. X.; and Wang, J. 2023. PDFFormer: propagation delay-aware dynamic long-range transformer for traffic flow prediction. In *Proceedings of the Thirty-Seventh AAAI Conference on Artificial Intelligence and Thirty-Fifth Conference on Innovative Applications of Artificial Intelligence and Thirteenth Symposium on Educational Advances in Artificial Intelligence, AAAI'23/IAAI'23/EAAI'23*. AAAI Press. ISBN 978-1-57735-880-0.

Krizhevsky, A.; Sutskever, I.; and Hinton, G. E. 2012. ImageNet Classification with Deep Convolutional Neural Networks. In Pereira, F.; Burges, C.; Bottou, L.; and Weinberger, K., eds., *Advances in Neural Information Processing Systems*, volume 25. Curran Associates, Inc.

Li, F.; Feng, J.; Yan, H.; Jin, G.; Yang, F.; Sun, F.; Jin, D.; and Li, Y. 2023. Dynamic Graph Convolutional Recurrent Network for Traffic Prediction: Benchmark and Solution. *ACM Trans. Knowl. Discov. Data*, 17(1).

Li, Y.; Yu, R.; Shahabi, C.; and Liu, Y. 2018. Diffusion Convolutional Recurrent Neural Network: Data-Driven Traffic Forecasting. In *6th International Conference on Learning Representations, ICLR 2018, Vancouver, BC, Canada, April 30 - May 3, 2018, Conference Track Proceedings*. OpenReview.net.

Liu, L.; Zhen, J.; Li, G.; Zhan, G.; He, Z.; Du, B.; and Lin, L. 2020. Dynamic spatial-temporal representation learning for traffic flow prediction. *IEEE Transactions on Intelligent Transportation Systems*, 22(11): 7169–7183.

Luetkepohl, H. 2005. *The New Introduction to Multiple Time Series Analysis*. ISBN 978-3-540-40172-8.

Lv, Y.; Duan, Y.; Kang, W.; Li, Z.; and Wang, F.-Y. 2015. Traffic Flow Prediction With Big Data: A Deep Learning Approach. *IEEE Transactions on Intelligent Transportation Systems*, 16(2): 865–873.

Ma, J.; Zhao, J.; and Hou, Y. 2024. Spatial-Temporal Transformer Networks for Traffic Flow Forecasting Using a Pre-Trained Language Model. *Sensors*, 24(17).

Pan, Z.; Ke, S.; Yang, X.; Liang, Y.; Yu, Y.; Zhang, J.; and Zheng, Y. 2021. AutoSTG: Neural Architecture Search for Predictions of Spatio-Temporal Graph. In *Proceedings of the Web Conference 2021, WWW '21*, 1846–1855. New York, NY, USA: Association for Computing Machinery. ISBN 9781450383127.

Qin, Y.; Fang, Y.; Luo, H.; Zeng, L.; Zhao, F.; and Wang, C. 2021. STformer: A Noise-Aware Efficient Spatio-Temporal Transformer Architecture for Traffic Forecasting.

Shao, Z.; Bell, M. G. H.; Wang, Z.; Geers, D. G.; Xi, H.; and Gao, J. 2024a. ST-Mamba: Spatial-Temporal Selective State Space Model for Traffic Flow Prediction. arXiv:2404.13257.

Shao, Z.; Bell, M. G. H.; Wang, Z.; Geers, D. G.; Yao, X.; and Gao, J. 2024b. CCDSReFormer: Traffic Flow Prediction with a Criss-Crossed Dual-Stream Enhanced Rectified Transformer Model. arXiv:2403.17753.

Shao, Z.; Wang, Z.; Yao, X.; Bell, M. G.; and Gao, J. 2025a. ST-MambaSync: Complement the power of Mamba and Transformer fusion for less computational cost in spatial-temporal traffic forecasting. *Information Fusion*, 117: 102872.

Shao, Z.; Xi, H.; Hensher, D. A.; Wang, Z.; Gong, X.; and Gao, J. 2025b. A spatial-temporal dynamic attention based Mamba model for multi-type passenger demand prediction in multimodal public transit systems.

Shao, Z.; Xi, H.; Lu, H.; Wang, Z.; Bell, M. G. H.; and Gao, J. 2024c. STLLM-DF: A Spatial-Temporal Large Language Model with Diffusion for Enhanced Multi-Mode Traffic System Forecasting. arXiv:2409.05921.

Smola, A.; and Schölkopf, B. 2004. A tutorial on support vector regression. *Statistics and Computing*, 14: 199–222.

Song, C.; Lin, Y.; Guo, S.; and Wan, H. 2020. Spatial-temporal synchronous graph convolutional networks: A new framework for spatial-temporal network data forecasting. In *Proceedings of the AAAI Conference on Artificial Intelligence*, volume 34, 914–921.

Vaswani, A.; Shazeer, N.; Parmar, N.; Uszkoreit, J.; Jones, L.; Gomez, A. N.; Kaiser, L. u.; and Polosukhin, I. 2017. Attention is All you Need. In Guyon, I.; Luxburg, U. V.; Bengio, S.; Wallach, H.; Fergus, R.; Vishwanathan, S.; and Garnett, R., eds., *Advances in Neural Information Processing Systems*, volume 30.

Wang, J.; Jiang, W.; and Jiang, J. 2023. LibCity-Dataset: A Standardized and Comprehensive Dataset for Urban Spatial-temporal Data Mining. *Intelligent Transportation Infrastructure*, liad021.

Wu, C.-H.; Ho, J.-M.; and Lee, D.-T. 2004. Travel-time prediction with support vector regression. *IEEE Transactions on Intelligent Transportation Systems*, 5(4): 276–281.

Wu, Z.; Pan, S.; Long, G.; Jiang, J.; Chang, X.; and Zhang, C. 2020. Connecting the Dots: Multivariate Time Series

Forecasting with Graph Neural Networks. KDD '20. New York, NY, USA: Association for Computing Machinery. ISBN 9781450379984.

Wu, Z.; Pan, S.; Long, G.; Jiang, J.; and Zhang, C. 2019. Graph Wavenet for Deep Spatial-Temporal Graph Modeling. In *IJCAI*.

Xu, Z.; Wei, X.; Hao, J.; Han, J.; Li, H.; Liu, C.; Li, Z.; Tian, D.; and Zhang, N. 2024. DGFormer: a physics-guided station level weather forecasting model with dynamic spatial-temporal graph neural network. *GeoInformatica*, 28: 1–35.

Yu, B.; Yin, H.; and Zhu, Z. 2018. Spatio-Temporal Graph Convolutional Networks: A Deep Learning Framework for Traffic Forecasting. In *IJCAI*.

Zhang, J.; Zheng, Y.; and Qi, D. 2016. Deep Spatio-Temporal Residual Networks for Citywide Crowd Flows Prediction. *Proceedings of the AAAI Conference on Artificial Intelligence*, 31.

Zhang, X.; and Zhao, J. 1998. Short-term traffic flow forecasting using fuzzy logic system methods. *Transportation Research Part C: Emerging Technologies*, 6(3): 187–206.

Zhao, J.; Zhuo, F.; Sun, Q.; Li, Q.; Hua, Y.; and Zhao, J. 2024. DSFormer-LRTC: Dynamic Spatial Transformer for Traffic Forecasting With Low-Rank Tensor Compression. *IEEE Transactions on Intelligent Transportation Systems*, PP: 1–13.

Zheng, C.; Fan, X.; Wang, C.; and Qi, J. 2020a. GMAN: A Graph Multi-Attention Network for Traffic Prediction. In *The Thirty-Fourth AAAI Conference on Artificial Intelligence, AAAI 2020, The Thirty-Second Innovative Applications of Artificial Intelligence Conference, IAAI 2020, The Tenth AAAI Symposium on Educational Advances in Artificial Intelligence, EAAI 2020, New York, NY, USA, February 7-12, 2020*, 1234–1241. AAAI Press.

Zheng, C.; Fan, X.; Wang, C.; and Qi, J. 2020b. GMAN: A Graph Multi-Attention Network for Traffic Prediction. *Proceedings of the AAAI Conference on Artificial Intelligence*, 34: 1234–1241.

Zhou, B.; He, D.; and Sun, Z. 2006. Traffic modeling and prediction using ARIMA/GARCH model. *Modeling and Simulation Tools for Emerging Telecommunication Networks: Needs, Trends, Challenges and Solutions*, 101–121.

Reproducibility Checklist

This paper:

- Includes a conceptual outline and/or pseudocode description of AI methods introduced (yes/partial/no/NA)

Answer: [Yes]

Justification: We have included a conceptual outline and pseudocode description of AI methods introduced.

- Clearly delineates statements that are opinions, hypothesis, and speculation from objective facts and results (yes/no)

Answer: [Yes]

Justification: We have clearly delineates statements that are opinions, hypothesis, and speculation from objective facts and results.

- Provides well marked pedagogical references for less-familiar readers to gain background necessary to replicate the paper (yes/no)

Answer: [Yes]

Justification: We have provides well marked pedagogical references for less-familiar readers to gain background necessary to replicate the paper.

Does this paper make theoretical contributions? (yes/no)

Answer: [No]

If yes, please complete the list below.

- All assumptions and restrictions are stated clearly and formally. (yes/partial/no)
- All novel claims are stated formally (e.g., in theorem statements). (yes/partial/no)
- Proofs of all novel claims are included. (yes/partial/no)
- Proof sketches or intuitions are given for complex and/or novel results. (yes/partial/no)
- Appropriate citations to theoretical tools used are given. (yes/partial/no)
- All theoretical claims are demonstrated empirically to hold. (yes/partial/no/NA)
- All experimental code used to eliminate or disprove claims is included. (yes/no/NA)

Does this paper rely on one or more datasets? (yes/no)

Answer: Yes

Justification: We rely on more datasets.

If yes, please complete the list below.

- A motivation is given for why the experiments are conducted on the selected datasets (yes/partial/no/NA)

Answer: [Yes]

Justification: We have given the motivation why the experiments are conducted on the selected datasets.

- All novel datasets introduced in this paper are included in a data appendix. (yes/partial/no/NA)

Answer: [NA]

Justification: This paper does not introduce any novel datasets; all experiments are conducted on publicly available datasets.

- All novel datasets introduced in this paper will be made publicly available upon publication of the paper with

a license that allows free usage for research purposes. (yes/partial/no/NA)

Answer:[NA]

Justification: This paper does not introduce any novel datasets; all experiments are conducted on publicly available datasets.

- All datasets drawn from the existing literature (potentially including authors' own previously published work) are accompanied by appropriate citations. (yes/no/NA)

Answer:[Yes]

Justification: We have cited appropriate citations of all datasets drawn from the existing literature (potentially including authors' own previously published work).

- All datasets drawn from the existing literature (potentially including authors' own previously published work) are publicly available. (yes/partial/no/NA)

Answer:[Yes]

Justification: We have cited appropriate citations of all datasets drawn from the existing literature (potentially including authors' own previously published work).

- All datasets that are not publicly available are described in detail, with explanation why publicly available alternatives are not scientifically satisfying. (yes/partial/no/NA)

Answer:[No]

Justification: We do not have any undisclosed datasets.

Does this paper include computational experiments? (yes/no)

Answer:[Yes]

Justification: This paper includes computational experiments.

If yes, please complete the list below.

- Any code required for pre-processing data is included in the appendix. (yes/partial/no).

Answer:[Yes]

- All source code required for conducting and analyzing the experiments is included in a code appendix. (yes/partial/no)

Answer:[Yes]

Justification: We have included the code in the supplementary materials.

- All source code required for conducting and analyzing the experiments will be made publicly available upon publication of the paper with a license that allows free usage for research purposes. (yes/partial/no)

Answer:[Yes]

Justification: We will make all source code required for conducting and analyzing the experiments publicly available upon publication of the paper with a license that allows free usage for research purposes.

- All source code implementing new methods have comments detailing the implementation, with references to the paper where each step comes from (yes/partial/no)

Answer:[Yes]

Justification: We have comments detailing the implementation of all source code implementing new methods, with references to the paper where each step comes from.

- If an algorithm depends on randomness, then the method used for setting seeds is described in a way sufficient to allow replication of results. (yes/partial/no/NA)

Answer:[Yes]

Justification: We have described the method used for setting seeds in a way sufficient to allow replication of results.

- This paper specifies the computing infrastructure used for running experiments, including GPU/CPU models; amount of memory; operating system; names and versions of relevant software libraries and frameworks. (yes/partial/no)

Answer:[Yes]

Justification: We have specified the computing infrastructure used for running experiments, including GPU/CPU models; amount of memory; operating system; names and versions of relevant software libraries and frameworks.

- This paper formally describes evaluation metrics used and explains the motivation for choosing these metrics. (yes/partial/no)

Answer:[Yes]

Justification: We have formally described the evaluation metrics used and explained the motivation for choosing these metrics.

- This paper states the number of algorithm runs used to compute each reported result. (yes/no)

Answer:[Yes]

Justification: We have stated the number of algorithm runs used to compute each reported result.

- Analysis of experiments goes beyond single-dimensional summaries of performance (e.g., average; median) to include measures of variation, confidence, or other distributional information. (yes/no)

Answer:[No]

Justification: While we did not explicitly report measures such as standard deviation or confidence intervals, our experimental evaluation spans multiple datasets, diverse traffic settings, and a variety of metrics (MAE, RMSE, MAPE). We also conducted comprehensive ablation studies and visual analyses (e.g., error heatmaps, module-wise outputs) to demonstrate robust and consistent improvements. These analyses help ensure that the observed performance gains are not limited to single conditions and reflect generalizable trends across different scenarios.

- The significance of any improvement or decrease in performance is judged using appropriate statistical tests (e.g., Wilcoxon signed-rank). (yes/partial/no)

Answer:[No]

Justification: While we did not apply formal statistical significance tests such as the Wilcoxon signed-rank test, we conducted comprehensive ablation studies across multiple datasets and metrics. These consistently demonstrated the effectiveness of each proposed component and supported the robustness of the observed improvements.

- This paper lists all final (hyper-)parameters used

for each model/algorithm in the paper's experiments.

(yes/partial/no/NA)

Answer:[partial]

Justification: In the experimental section, we described our hyperparameters.

- This paper states the number and range of values tried per (hyper-) parameter during development of the paper, along with the criterion used for selecting the final parameter setting. (yes/partial/no/NA)

Answer:[Partial]

Justification: We report the final hyperparameter settings used in our experiments, including batch size, optimizer, learning rate, scheduler, early stopping, and seed.